Vision-Based Mobile Indoor Assistive Navigation Aid for Blind People

Bing Li, *Member, IEEE*, Juan Pablo Muñoz, *Member, IEEE*, Xuejian Rong, Qingtian Chen, Jizhong Xiao, *Senior Member, IEEE*, Yingli Tian, *Fellow, IEEE*, Aries Arditi, and Mohammed Yousuf

Abstract—This paper presents a new holistic vision-based mobile assistive navigation system to help blind and visually impaired people with indoor independent travel. The system detects dynamic obstacles and adjusts path planning in real-time to improve navigation safety. First, we develop an indoor map editor to parse geometric information from architectural models and generate a semantic map consisting of a global 2D traversable grid map layer and context-aware layers. By leveraging the visual positioning service (VPS) within the Google Tango device, we design a map alignment algorithm to bridge the visual area description file (ADF) and semantic map to achieve semantic localization. Using the on-board RGB-D camera, we develop an efficient obstacle detection and avoidance approach based on a time-stamped map Kalman filter (TSM-KF) algorithm. A multi-modal human-machine interface (HMI) is designed with speech-audio interaction and robust haptic interaction through an electronic SmartCane. Finally, field experiments by blindfolded and blind subjects demonstrate that the proposed system provides an effective tool to help blind individuals with indoor navigation and wayfinding.

Index Terms—Indoor assistive navigation, semantic maps, obstacle avoidance, Google Tango device, blind and visually impaired people

✦

1 INTRODUCTION

ACCORDING to multiple federal and state civil rights laws in the United States, public areas such as airports and subway stations, need to accommodate the services and facilities accessibility for individuals with disabilities. Independent travel is always a daily challenge to those who are blind or visually impaired. According to the World Health Organization fact sheet as of October 2017, there were 6 million people who are blind and 217 million who have low vision worldwide [1].

Intelligent assistive navigation is an emerging research focus for the robotics community to improve the mobility of blind and visually impaired people. For indoor navigation on mobile devices, numerous studies have been carried out

in the past decades, such as using wireless sensor network fingerprints [2], [3], [4], [5], [6], [7], [8], geomagnetic fingerprints [9], inertial measurement unit [10], and Google Glass device camera [11], [12].

There are multiple challenges for mobile indoor assistive navigation: the inaccessibility of indoor positioning, the immature spatial-temporal modeling approaches for indoor maps, the lack of low-cost and efficient obstacle avoidance and path planning solutions, and the complexity of a holistic system on a compact and portable mobile device for blind users.

The advancements in computer vision software (such as visual odometry) and hardware (such as graphics processing units) in recent years have provided the potential capabilities for vision-based real-time indoor simultaneous localization and mapping (SLAM).

As more and more indoor venue map data becomes available on public maps (e.g., Google Maps, HERE Maps and AutoNavi Maps), the integration of context-aware information becomes essential for navigation systems. User-centered ambient contextual data allows a system to anticipate a user's personalized needs, and to customize his/her navigation experience. In this research, the indoor map with spatial context-aware information is referred to as *semantic map* for assistive blind navigation purposes.

In response to safety concerns, vision cameras have become more popular than other sensors (e.g., Sonar, Radar, and LIDAR) for obstacle detection and avoidance, thanks to its low cost and rich information in environments with proper lighting conditions. Monocular, stereo, and depth cameras have been widely used for object detection and tracking.

This paper summarizes our research work on novel intelligent situation awareness and navigation aid (ISANA) with an electronic SmartCane prototype that provides a holistic

- B. Li, X. Rong, and Q. Chen are with the Department of Electrical Engineering, City College (CCNY), City University of New York, 160 Convent Ave, New York, NY 10031.
  E-mail: {bli, xrong}@ccny.cuny.edu, qchen23@citymail.cuny.edu.
- J.P. Muñoz is with the Department of Computer Science, Graduate Center, City University of New York, 365 5th Ave, New York, NY 10016.
  E-mail: jmunoz2@gradcenter.cuny.edu.
- J. Xiao is with the CCNY Robotics Lab, Department of Electrical Engineering, City College, City University of New York, 160 Convent Ave, New York, NY 10031. E-mail: jxiao@ccny.cuny.edu.
- Y. Tian is with the CCNY Media Lab, Department of Electrical Engineering, City College, City University of New York, 160 Convent Ave, New York, NY 10031. E-mail: ytian@ccny.cuny.edu.
- A. Arditi is with Visibility Metrics LLC, 49 Valley View Road, Chappaqua, NY 10514. E-mail: arditi@visibilitymetrics.com.
- M. Yousuf is with the Federal Highway Administration, Washington, DC 20590. E-mail: Mohammed.Yousuf@dot.gov.

Fig. 1. Proposed intelligent situation awareness and navigation aid (ISANA) system field demo at the U.S. Department of Transportation (DOT) headquarter buildings in Washington, D.C. News.

solution for indoor assistive navigation. The system uses the Google Tango tablet[1] as its mobile computing platform.

The main contributions of this research are as follows:

1) We proposed a real-time holistic mobile solution called ISANA for blind navigation and wayfinding, which was successfully demonstrated in U.S. DOT headquarter buildings (as shown in Fig. 1), and achieved greater success than previous efforts.

2) We developed the CCNY indoor map editor to parse geometric information from architectural CAD models and extract the semantic map with a global 2D traversable grid map layer and context-aware layers which enabled the global path planning to desired destinations.

3) We presented an efficient obstacle detection and avoidance method that not only augments navigation safety but also adjusts the path in real-time.

4) We designed the CCNY SmartCane for robust HMI which mitigates the problems caused by non-perfect voice recognition software, such as malfunctions in noisy environments or command misunderstanding from users with accents.

The remainder of this paper is organized as follows. Section 2 reviews various vision-based indoor assistive navigation systems, context-aware approaches, and obstacle avoidance research. Section 3 presents an overview of the ISANA system and the high-level relationships among different modules. Section 4 elaborates the pipeline to construct semantic maps using the indoor map editor. Section 5 presents obstacle detection and motion estimation approaches using TSM-KF. Section 6 elaborates the multi-modal HMI design. Section 7 shows the quantitative and qualitative experimental evaluations. Finally, Section 8 concludes the paper and discusses the future research directions.

2 RELATED WORK

2.1 Vision-Based Indoor Assistive Navigation

Advancements in computer vision provide the capabilities to support assistive navigation in real-time. In some research, vision cameras have been utilized for assistive navigation systems in several variants, including monocular [11], [12], stereo [13], fish-eye [14], omni-directional [15] and RGB-D [16].

The University of Southern California stereo system [13] was an early wearable prototype with navigation and obstacle detection functionalities. It installed a head-mounted

vision sensor and a haptic feedback actuator. Stereo visual odometry was performed by matching features across two stereo views, and visual SLAM was performed subsequently. Obstacles were detected using stereo point cloud processing and were represented in the visual odometry coordinate frame. The system alerted the user when obstacles were detected in front. However, the system lacked obstacle modeling in a global map representation during navigation, such that dynamic path planning was not supported for real-time obstacle avoidance.

With rapid growth and evolution of mobile technology, mobile indoor assistive navigation systems have drawn enormous attentions among researchers in recent years. The Navatar project [11] employed an inertial measurement unit (IMU) in a smart mobile device (Google Glass) for ego-motion estimation. The user of Navatar was required to confirm the presence of landmarks such as corners and doors for indoor localization. However, this user-as-sensor approach was undesirable since it increased the cognitive load of the blind user. Also, Navatar was incapable of performing obstacle avoidance.

The Google Tango device has been recently explored to augment indoor mobility and safety for blind and visually impaired users. Researchers at Illinois State University presented their system called Cydalion [17]. Cydalion uses depth perception to detect obstacles and head-level objects, and it provides audio tones and haptic feedback for the user. Although Cydalion makes a commendable attempt for the safety concerns using obstacle detection, it is not able to provide global navigation guidance for the user. Also, Cydalion is purely relying on the audio feedback and does not support haptic interaction. Researchers and developers from Cologne Intelligence also developed an augmented reality solution for the indoor navigation [18]. The system shows a navigation path overlaid on the 2D camera view. Nonetheless, the system is unable to perform obstacle avoidance with dynamic path planning, and there is no decent HMI for the user.

2.2 Context-Aware Approaches

The notion of "Context-Aware Computing" was introduced in the early 90s [19], and it was first described as an approach to customize user experience according to his/her spatial location, the collection of nearby people, hosts, accessible devices, and the changes of all these contextual information over time. The spatial reasoning was later added in the assistive navigation in an intelligent wheelchair project [20], and it used the semantic information to augment navigation and situation awareness.

A context-aware indoor navigation system was presented for user-centric path planning to help people find their destinations according to their preferences and contextual information [21], [22]. This user model included various information about physical capabilities, access rights, and user preference modeling. The system used a hybrid model of the indoor map representation which combines symbolic graph-based models and geometric models.

Knowledge representation and management for context-aware indoor mobile navigation has been presented by Afyouni [23], [24]. The spatial query was designed and implemented using PostgreSQL database management system.

Fig. 2. ISANA and SmartCane system configuration on a blindfolded sighted subject.

Fig. 3. ISANA system functional block diagram.

Considering user-centric contextual dimensions and mobile data management issues, a hierarchical feature-based indoor spatial data model was presented by taking into account additional contextual data such as time, user profiles, user preferences and real-time events. However, this framework was not specifically designed for blind navigation.

2.3 Obstacle Avoidance Approaches

Navigation capability and safe travel are essential for indoor assistive navigation systems. Real-time obstacle avoidance is a particular challenge for autonomous robotic systems. Researchers have explored various obstacle avoidance strategies for autonomous navigation.

As the pioneering effort of indoor robotic navigation, NavChair used sonar sensor to detect objects. A vector field histogram (VFH) algorithm [25] and later Minimal VFH [26] were proposed to provide effective sonar-based obstacle detection and avoidance. VFH used sonar readings to update a local map with detected obstacle in the form of uncertainty grids, which was used to calculate a polar histogram to represent the geometric information of the obstacles. Finally, NavChair found a direction with minimum VFH cost and followed it to bypass obstacles.

Depth maps from stereo-vision systems have been used for the detection of obstacle-free space in autonomous robotic systems. CASBliP developed a blind navigation system to fuse different information sources to help visually impaired users to deal with mobility challenges [27]. Based on the assumption that obstacle-free pathway is at the bottom of the depth image, CASBliP detects the obstacle-free pathway as the bottom partition of the image which has small disparities. However, this assumption does not hold for robust safety, and CASBliP is not able to perform dynamic path planning to avoid obstacles.

The RGB-D indoor navigation system from the University of Southern California for blind people can perform global obstacle avoidance during assistive navigation [28]. Based on the visual odometry using a glass-mounted RGB-D camera, the system first built a 3D voxel map of the environment, and a 2D probabilistic occupancy map was updated in r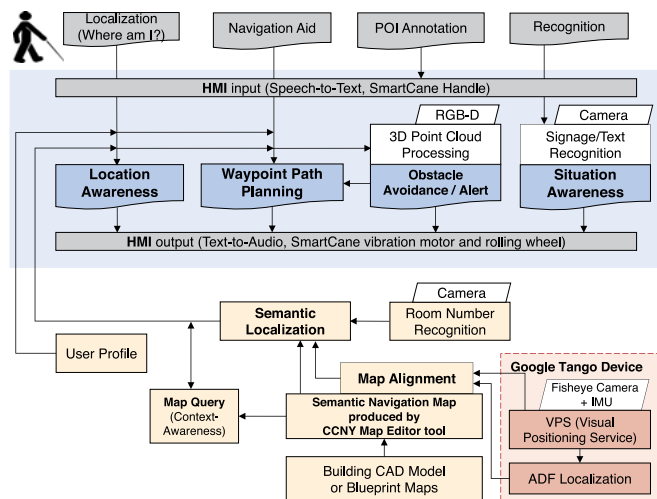eal-time. Three grid states (occupied, free, and unknown) were represented in the global 2D traversable grid map to support dynamic path planning. Nonetheless, this traversable map lost the vertical geometric information of the obstacles. Therefore, the system was not able to detect some obstacles, such as head-level objects.

Using Tango device, obstacle detection and avoidance approaches have been developed based on depth image [29], [30]. The edge detector was first used to remove all edges, and a connected component algorithm extracted all connected regions such as the floor at the bottom of the image. The non-floor image region was segmented into three sections for local obstacle avoidance guidance: bear right, bear left, and no clear path [29]. However, this approach can only detect and avoid obstacles locally and cannot do global path planning.

3 SYSTEM OVERVIEW

The proposed ISANA system runs on Google Tango mobile device, which has an embedded RGB-D camera providing depth information, a wide-angle camera for visual motion tracking, and a 9-axis inertial measurement unit for visual-inertial odometry. The physical configuration of the prototype is shown in Fig. 2, which includes a Tango tablet, a frame holder, and a SmartCane which outfits a keypad and two vibration motors on a standard white cane. ISANA provides indoor wayfinding guidance for blind users with location context awareness, obstacle detection and avoidance, and robust multi-modal HMI.

We leverage the Tango VPS and ADF for ISANA assistive navigation, as shown in the bottom right of the system functional block diagram in Fig. 3. Fast retina keypoint visual features [31] are extracted from the wide-angle camera for six degrees of freedom (DOF) visual odometry (VO), which is fused with IMU for visual-inertial odometry (VIO). The visual feature model is stored in ADF for loop closure detection so that the accumulated odometry drift can be suppressed.

The indoor semantic map and localization play fundamental roles for ISANA, as shown in the bottom part of Fig. 3. Based on the CAD model (or blueprint maps) as the input, the indoor map editor constructs the semantic map with multiple geometric layers (Section 4), such as global 2D traversable grid map layer and point/area of interest layers (POI and AOI), and topological layers. Then, the
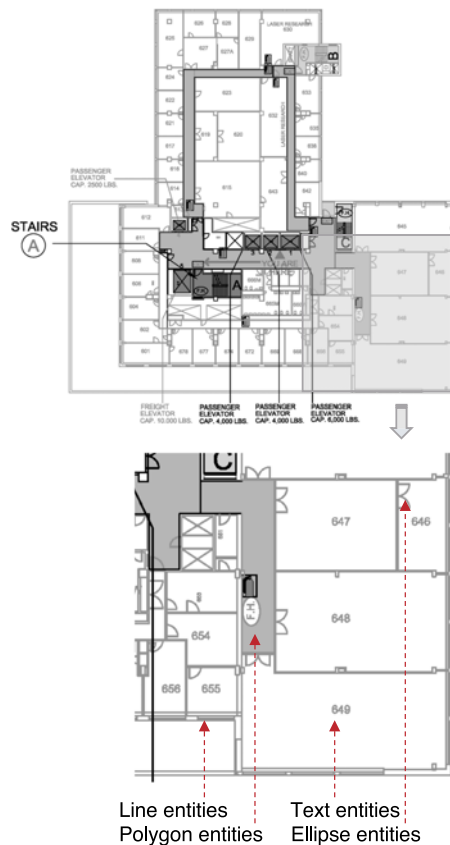
Fig. 4. CAD model floor map example used in the experiment. It includes various geometric layer entities: Line entities represent the layout, polygon entities for walkable hallways, ellipse entities for doors, and text entities for room number labeling.
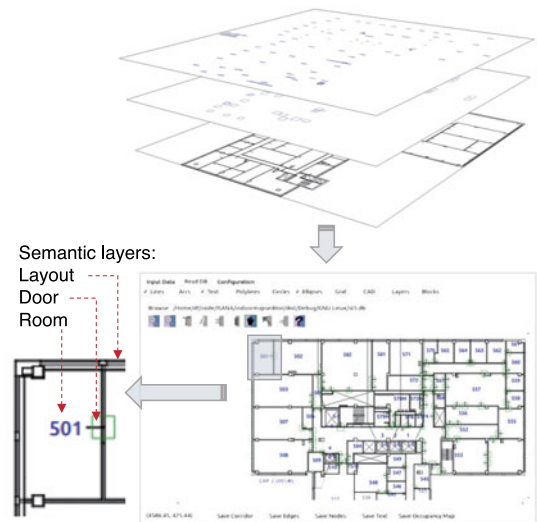

Fig. 5. Semantic layers extracted from CAD model using our indoor map editor. The layout is parsed from line entities, the doors are from ellipse entities, and the rooms are from text entities. Polygon entities are not applied due to it deficient representation for the hallway areas.

geometric layers are aligned with Tango ADF using the approach elaborated in Section 4.3. Therefore, ISANA achieves *semantic localization* to localize the user on the semantic map for path planning and location awareness.

To provide cognitive guidance for blind users, a novel way-point path planner [32] is implemented in ISANA based on A* algorithm and post-processing path pruning. To address safety concerns during navigation, a real-time obstacle detection approach is efficiently designed to provide the user both dynamic path planning and local obstacle avoidance using the on-board RGB-D sensor data. Signage and text recognition is also built into ISANA for situation awareness [33].

A multi-modal human-machine interface (HMI) handles the interaction between ISANA and blind users. To cope with the conflicts of information delivery and user cognitive load, we minimize the audio announcements using event triggering. A multi-priority mechanism is designed for audio announcements to ensure higher priority messages can be conveyed on time. An electronic SmartCane is designed [34] to provide a complementary HMI through tactile input and vibration feedback, and it is especially useful in noisy environments, where speech recognition is not robust.

4 INDOOR SEMANTIC MAPS AND LOCALIZATION

4.1 Architectural Model Data

Computer-Aided Design (CAD), such as in drawing interchange format (DXF), is a common model for architectural drawings. Instead of creating all semantic information

manually, retrieving geometric layers from CAD model is more efficient.

Our indoor map editor parses the DXF file and extracts spatial geometric information about the building floors, such as polygon entities, ellipse entities, line entities and text entities. Fig. 4 shows a typical CAD model that is used for experimental evaluation.

There are two fundamentally different representations for architectural data modeling: Computer-Aided Design and Building Information Modeling (BIM). As two-dimensional electronic drawings, CAD models consist of 2D graphic elements such as lines, ellipses, and texts. Indoor BIM is a more comprehensive model that provides useful semantic information (e.g., walls, windows, rooms and space connections) that can be used for indoor navigation purposes. Although we recognize the benefit of 3D BIM data, in this paper we focus on the CAD model data since it is available for most existing buildings.

According to the CAD Standards, the DXF file includes (but is not limited to) the following entities and attributes:

1) Layering (organized in the hierarchy) and colors
2) Units and scale factors
3) Line (or polyline) types and line weights
4) Arc types and directions
5) Text style, font, and size
6) Room and door numbering
7) Title block and sheet titles
8) Drawing sequence and sheet numbers

4.2 Semantic Map Construction

We automated the map generation process by developing an indoor map editor to parse the CAD model of architectural floor map, which was provided by the CCNY Campus Planning and Facilities Management department. The map editor parses the DXF file using Dxflib library, and extracts the geometric entities of the floor's model, including line entities, text entities, polygon entities, and ellipse entities, as shown in Fig. 5.
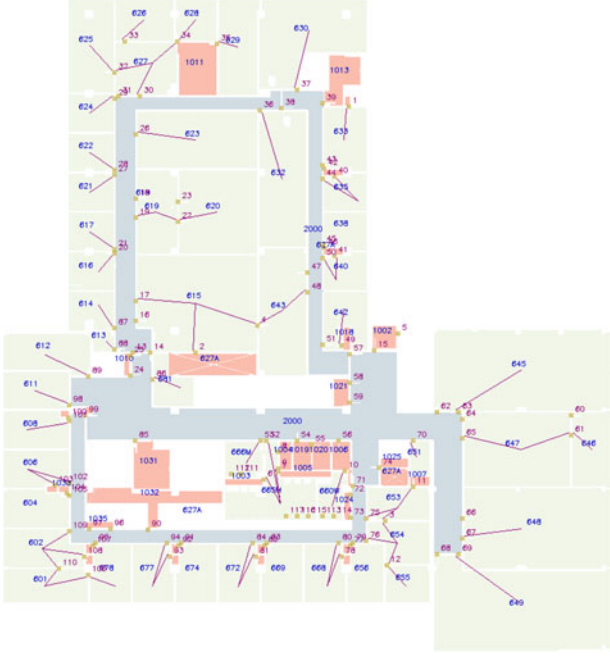
Fig. 6. Retrieved topological map with semantic information [35]. The red topological lines on the top show the connectivities between room labels, doors, and hallways. On the background, the green denotes the area of each room, the blue shows the hallways which are connecting with at least a threshold number of doors, and the red shows the unknown spaces.

Algorithm 1. Semantic Extraction Based on Prim's MST Algorithm

 Input:
  I: layout image created from CAD layers (Fig. 5)
  rL: room points list
  dL: door points list
 Output: (Fig. 6)
  h: global 2D traversable grid map
  g: semantic topology graph, context-aware layers
1: **procedure** SEMANTICCONSTRUCTIONI, rL, dL
  ▷ create G as adjacency list from I
2: $G_{V,E} \leftarrow adjList(I)$, $g \leftarrow empty$
3: $h \leftarrow image(I.width, I.height)$ as $WHITE$
4: **for** each s in rL, then in dL **do**
5: $g.vertex.add(s)$ ▷ add it as source vertex
6: $Va \leftarrow G_{BLACK}$, $Va[s] \leftarrow WHITE$ ▷ vertex visited array
7: $Pq \leftarrow INFINITY$ ▷ priority queue initial value
8: $Q \leftarrow s$ ▷ priority queue
9: $Ad \leftarrow NULL$ ▷ adjacency list
10: **while** $(Q! = empty)$ **do** ▷ Prim's MST algorithm
11:   $m \leftarrow minimum\_weight(Pq)$
12:   **for** v in $neighbor\_of(m)$ **do**
13:    $update\ Q, Va, Pq, Ad$
14:    $g \leftarrow edge(room, door)$
15:    $h[s.i, s.j] \leftarrow GREEN$ ▷ room areas
16:    **if** $door\_no(g_s.vertex) > DOOR\_MIN$ **then**
17:     $h[s.i, s.j] \leftarrow DARK\_BLUE$ ▷ hallway areas
18:    **else if** $g_s.vertex$ not in rL **then**
19:     $h[s.i, s.j] \leftarrow RED$ ▷ unknown areas
20: **return** (g, h)

Further, our indoor map editor recognizes the regions of hallways, the topologies between room labels and corresponding doors, the global 2D traversable grid map layer,
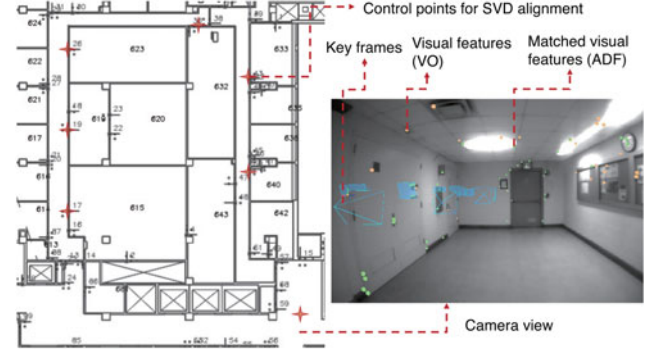

Fig. 7. Indoor semantic map and ADF map alignment using SVD [35]. The left part is the semantic map with geometric layers and the control points, which are arbitrarily selected and are shown as the red starts. The right part shows the ADF features in a keyframe.

room area and labels, door locations. In addition, the map editor is able to edit (add or delete) any semantic information, such as connectors (e.g., elevator banks and stairs) between floors to support multi-floor transitions. All of this spatial context-aware information is referred to as the semantic map to support assistive navigation and location awareness purposes.

To retrieve the semantic information, a lattice graph is introduced to model the architectural layout image with nodes and edges corresponding to vertices between adjacent nodes, as an undirected graph $G = (V, E)$. Then, the region growing process to find each room is modeled as a minimum spanning tree (MST) problem. MST is the spanning tree (a subgraph containing every vertex of G) minimizing the total weight.

As shown in Algorithm 1, ISANA first constructs the adjacency list from the global 2D traversable grid map. Next, an automated region growing approach using Prim's algorithm is performed to find all rooms, as well as all topological connections between room labels and their connecting doors, with the computational complexity of $O((V + E)logV)$ using adjacency list representation.

Then, the hallways are retrieved as regions which have more than certain number connecting doors (the threshold is chosen as 10 for our experiment). Finally, any other spaces which are not connecting with doors or room labels are recognized as unknown areas. The result is shown in Fig. 6.

4.3 Map Alignment for Semantic Localization

The map alignment and semantic localization are performed on the Tango mobile device by a sighted person. The Tango VPS provides 6-DOF pose estimation based on visual odometry and ADF features, which are understandable only by computer algorithms. However, blind users and ISANA need the semantic map to understand the scene for navigation purposes through graphical user interface (GUI) and human-machine interaction. Furthermore, the global 2D traversable grid map layer is required for the path planning algorithm.

Therefore, to establish the spatial relationship between the ADF feature map and the semantic map, we proposed a novel alignment algorithm so that ISANA is able to localize the user in the semantic map.

Fig. 7 illustrates the concept of ADF and semantic navigation map alignment method, which selects a set of control

points on the semantic navigation map and the Tango device collects the ADF keyframe features in the real environment at the same physical positions as the control point set.

The alignment algorithm uses singular value decomposition (SVD) approach to find a homogeneous transformation matrix A, which projects Cartesian coordinate system of the ADF to the semantic map by aligning these two corresponding point sets for optimized least-squares sum.

A SVD approach is introduced to align the ADF and the semantic map. Let us denote $l_n = [x_n, y_n]^T \in L_{N \times 2}$ as the planar $\mathbb{R}^2$ coordinates of control point set from the Tango ADF local $\mathbb{R}^3$ coordinate system, and $p_n = [i_n, j_n]^T \in P_{N \times 2}$ as the corresponding point set on the semantic map. N is the number of control points, and n is the index.

The goal is to find the homogeneous transformation matrix A and it is composed by a rotation matrix $R_{2 \times 2}$ and a translation vector $t_{2 \times 1}$ as

$$(R, t) \leftarrow \arg\min_{R,t} \sum_{i=1}^{N} ||R\,p_i + t - l_i||^2 \tag{1}$$

and we denote $A = \begin{bmatrix} R_{2 \times 2} & t_{2 \times 1} \\ 0 & 1 \end{bmatrix}$.

Where the $R \in \Omega = \{R | R^T R = R R^T = I_2\}$, and Ω is the set of orthogonal rotation matrices.

By selecting a set of control points arbitrary distributed (rather than with a pattern like: on a line) in the semantic map, based on its corresponding control point set in ADF feature map, we have A as an over-constrained matrix, so that it guarantees the least-squares solution of Equation (1).

Equation (1) is linear with respect to t, but nonlinear with respect to R. We denote the centroid of L and P as $\bar{l} = \frac{1}{N} \sum_{n=1}^{N} l_i$, and $\bar{p} = \frac{1}{N} \sum_{n=1}^{N} p_i$, and introduce the matrices $\hat{L} = L - \bar{l}$ and $\hat{P} = P - \bar{p}$. Therefore, the problem can be represented as the below equivalent formulation

$$R \leftarrow \arg\min_{R} \sum_{i=1}^{N} ||R\,\hat{p}_i - \hat{l}_i||^2. \tag{2}$$

By defining A as Equation (3), we can transform Equation (1) into Equation (4)

$$A = \begin{bmatrix} cos(\theta) & -sin(\theta) & t_x \\ sin(\theta) & cos(\theta) & t_y \\ 0 & 0 & 1 \end{bmatrix} \tag{3}$$

$$Mx = b$$

$$M = \begin{bmatrix} x_1 & -y_1 & 1 & 0 \\ y_1 & x_1 & 0 & 1 \\ \vdots & \vdots & \vdots & \vdots \\ x_n & -y_n & 1 & 0 \\ y_n & x_n & 0 & 1 \end{bmatrix} \tag{4}$$

$$x = [cos(\theta), sin(\theta), t_x, t_y]^T$$

$$b = [i_1, j_1, \ldots, i_n, j_n]^T.$$

Considering the cross-covariance matrix M, we use the SVD to factorize it

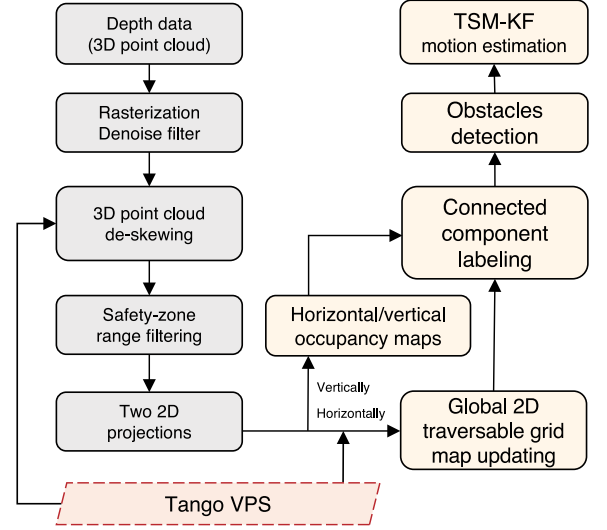$$M_{N \times 4} = U_{N \times N} S_{N \times 4} V_{4 \times 4}^T. \tag{5}$$

Fig. 8. Obstacle detection and motion estimation flowchart.

Where U includes the eigenvectors of MM^T, S is diagonal matrix with singular values σ_i, and V is the matrix with eigenvectors of $M^T M$. Finally we find the optimal values for Equation (1) by

$$x = (V diag(\sigma_1^{-1}, \ldots, \sigma_4^{-1}) U^T)^{-1} b. \tag{6}$$

5 NAVIGATION WITH OBSTACLE AVOIDANCE

In this section, we elaborate on the obstacle avoidance design to improve assistive navigation safety. Based on the global 2D traversable grid map layer in the semantic map, a global navigation graph is constructed and a path planner based on A^* algorithm is designed to generate a waypoint route for the user [36].

5.1 Obstacle Detection

The obstacle detection is performed using the RGB-D camera, and it runs efficiently in real-time on the Tango mobile device at 5 HZ.

As shown in the left part of Fig. 8, after the voxel rasterization, a denoise filter is performed to remove the outlier voxels. Rather than utilizing our previous approach [37] of random sample consensus (RANSAC) for floor segmentation, based on the roll and pitch information of the current pose, we perform an efficient de-skewing process to align the 3D voxels with the horizontal plane. Then, we applied a two 2D projection approach for obstacle avoidance.

In the middle block of Fig. 8, the horizontal projection creates a horizontal occupancy map for dynamic path planning, and the vertical projection creates a vertical occupancy map for obstacle alerts (visualized in Fig. 14). Since this occupancy map is with time stamps in every frame, we name it *time-stamped map (TSM)*. The whole detection process is efficient because its computational cost is determined by the granularity of the occupancy map rather than the number of the point cloud. The granularity is chosen according to the scale of the environment.

On the right part of Fig. 8, a connected component labeling approach [38] is designed for object detection on horizontal and vertical occupancy maps. Then, we choose a nearest spatial neighbor to identify each object in sequential

frames. The detection process is shown in Algorithm 2. Finally, every set of connected labels is grouped as an object.

Algorithm 2. Obstacle Detection Based on Connected Component Labeling Approach

---

Input:
    G: horizontal or vertical occupancy map
    b: background value
Output:
    obL: obstacle bounding box (position, size: [px, py, sx, sy]) list
1: **procedure** ObstacleDetectionG, b
2:    $L \leftarrow G$ ▷ initialization: Label
3:    $(W, H) \leftarrow L.size()$ ▷ initialization: Width, Height
4:    $childList, labelSet, label \leftarrow empty$
5:    **for** w, h in W, H **do**   ▷ label it
6:      **if** $L(w,h) != b$ **then**
7:        $update\ label$
8:        $L(w,h) \leftarrow label$
9:        $append\ L(w,h)\ to\ childList\ if\ its\ top/left\ exists$
10:   **for** w, h in W, H **do**   ▷ label updating
11:     **if** $L(w,h) != b$ **then**
12:       **if** $L(w,h)\ in\ childList$ **then**
13:         $update\ it\ as\ its\ father$
14:       **else**
15:         $add\ it\ in\ labelSet$
16:   **for** $label$ in $labelSet$ **do** ▷ get result
17:     $ob \leftarrow bounding\_box(label)$
18:     $append\ ob\ to\ obL$
19:   **return** obL

5.2 Obstacle Motion Estimation

After ISANA projects the detected obstacles in the horizontal occupancy map, an efficient Kalman filter (KF) is integrated to predict the motion of each obstacle to improve the navigation safety in the dynamic environment. For a detected object in sequential frames, its state X of the discrete-time process can be estimated by the linear stochastic differential equations

$$X_k = A_k X_{k-1} + w_{k-1}. \qquad (7)$$

And the measurement equation

$$Z_k = C_k X_k + v_k. \qquad (8)$$

A_k Matrix ($n \times n$) describes how the state evolves from $k-1$ to k without controls or noise. n is the dimension of the states.

C_k Matrix ($m \times n$) describes how to map the state X_k to an observation Z_k, where m is the vector size of the observation.

$w_{n \times 1}$ and $v_{m \times 1}$ are noise vectors representing the process and measurement noise respectively. The corresponding noise covariance matrices are denoted as $Q_k = cov(w_k, w_k) = E(w_k, w_k^T)$ and $R_k = cov(v_k, v_k) = E(v_k, v_k^T)$. The noise is assumed to be independent and normally distributed with the mean μ at zero, as $p(w) \sim \mathcal{N}(0, Q)$, $p(v) \sim \mathcal{N}(0, R)$.

The KF obstacle motion estimation based on TSM consists of two main processes: the prediction process and the update process. The algorithm starts by taking the inputs of the initial estimation of the system X_0 and its associated state covariance Σ_0. Based on these two values, the prediction process is first utilized to predict X and Σ. Then, the KF gain is updated and is fused with system measurement Z_k to estimate the next state X_k and state covariance Σ_k.

(1) Obstacle motion prediction
The state of an obstacle is selected as

$$X = \begin{bmatrix} px & py & vx & vy & sx & sy & svx & svy \end{bmatrix}^\mathsf{T}. \qquad (9)$$

Where px and py represent the mass center of this obstacle, and vx and vy are velocities of this obstacle in the x-direction and y-direction respectively. The sx and sy are the tracking window width and length (size), and svx and svy are the size change rates. Therefore, the prediction can be denoted as

$$\begin{cases} \hat{X}_k = A_k X_{k-1} + w_{k-1} \\ \hat{\Sigma}_k = A_k \Sigma_{k-1} A_k^\mathsf{T} + Q_k. \end{cases} \qquad (10)$$

By assuming zero mean acceleration model, the transition can be represented as

$$\begin{cases} px_k = px_{k-1} + vx_{k-1}\Delta t \\ py_k = py_{k-1} + vy_{k-1}\Delta t. \end{cases} \qquad (11)$$

Therefore, we get the state transition in Equation (12). Δt is assigned as the value of depth perception period

$$A_k = \begin{bmatrix} 1 & 0 & \Delta t & 0 & 0 & 0 & 0 & 0 \\ 0 & 1 & 0 & \Delta t & 0 & 0 & 0 & 0 \\ 0 & 0 & 1 & 0 & 0 & 0 & 0 & 0 \\ 0 & 0 & 0 & 1 & 0 & 0 & 0 & 0 \\ 0 & 0 & 0 & 0 & 1 & 0 & 0 & 0 \\ 0 & 0 & 0 & 0 & 0 & 1 & 0 & 0 \\ 0 & 0 & 0 & 0 & 0 & 0 & 1 & 0 \\ 0 & 0 & 0 & 0 & 0 & 0 & 0 & 1 \end{bmatrix}. \qquad (12)$$

The Kalman gain is calculated by

$$K_k = \hat{\Sigma}_k C_k^\mathsf{T} (C_k \hat{\Sigma}_k C_k^\mathsf{T} + R_k)^{-1}. \qquad (13)$$

(2) Obstacle motion correction
The obstacle position and size are measured in each camera frame, thus the observation can be represented as

$$\begin{cases} Z_k = \begin{bmatrix} px & py & sx & sy \end{bmatrix}^\mathsf{T} \\ Z_k = C_k X_k + v_k, \end{cases} \qquad (14)$$

where

$$C_k = \begin{bmatrix} 1 & 0 & 0 & 0 & 0 & 0 & 0 & 0 \\ 0 & 1 & 0 & 0 & 0 & 0 & 0 & 0 \\ 0 & 0 & 0 & 0 & 1 & 0 & 0 & 0 \\ 0 & 0 & 0 & 0 & 0 & 1 & 0 & 0 \end{bmatrix}. \qquad (15)$$

Finally, the object state vector and covariance are updated by

$$\begin{cases} X_k = \hat{X}_k + K_k(Z_k - C_k \hat{X}_k) \\ \Sigma_k = (I - K_k C_k)\hat{\Sigma}_k. \end{cases} \qquad (16)$$
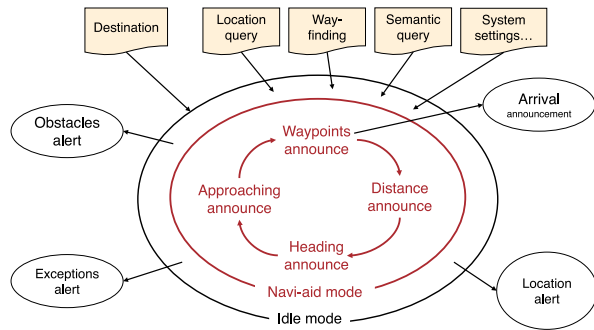
Fig. 9. ISANA operational mode and HMI.

5.3 Navigation with Obstacle Avoidance

ISANA performs obstacle detection and motion estimation to improve the navigation safety. The detected obstacles are initially represented in the horizontal and vertical occupancy maps. Further, after they are detected using the connected component labeling approach, the obstacle projection in the horizontal occupancy map is transformed to 2D global traversable grid map (visualized in Fig. 14) for real-time dynamic path planning.

During navigation, ISANA detects the front obstacles and estimates the motion model in the global 2D traversable grid map. For obstacles which block the route to the next waypoint or move towards the user, our path finder algorithm [36] updates the detected obstacles (or its predication) in the navigation graph and find a new path (as shown in experimental Section 7.3) to avoid the obstacles. For obstacles which are not conflicting with the planned route, ISANA only provides obstacle alerts.

6 HUMAN MACHINE INTERFACE

6.1 Operational Mode and Usability Study

ISANA works as a vision substitution for blind individuals to perform cognitive level waypoint navigation guidance. The human-machine interface is critical for good user experience. We conducted a user preferences and needs questionnaire in our previous research [39]. The survey results from blind community show that a human-in-the-loop methodology is preferred for the assistive electronic travel aid (ETA), and query-based interaction is preferred over a menu. The subjects prefer audio as the output media for navigating guidance. The priority list of the most environmental objects to be located in indoor navigation are: doors, stairs, furniture, persons, personal items, and event text signs. Also, according to a survey made by Golledge [40], tactile input (e.g., keypad or button) is preferred by the blind participants.

A human-in-the-loop HMI is designed for ISANA. The user is always in control, and ISANA adapts to the user's action and responses according to user's query. To effectively deliver rich semantic and guidance information while retaining robustness, a multi-modal HMI is designed for blind users with speech-audio as the main interaction modality, and with SmartCane for robust haptic interaction in noisy environments.

The operational mode of ISANA HMI is illustrated in Fig. 9. The small ellipses represent audio announcements or alerts, while the shaded command shapes indicate user inputs. ISANA HMI includes two operational modes: Idle

mode (outer ellipse) and Navi-aid mode (inner ellipse). The area between outer and inner ellipses are considered to be applicable for both modes.

After the system initialization and localization from VPS, ISANA enters the Idle mode. In this mode, the user can input navigation control commands, query location awareness, and configure ISANA settings. The event alerts include obstacle in front, system exceptions (e.g., the power of the system is below a threshold) and location alerts to announce POI/AOI, and the number of alerts is minimized to decrease the cognitive load for the user. To enter Navi-aid mode, the user just needs to specify a destination.

In the Navi-aid mode, a cognitive waypoint path (how many turns to the destination) is computed by ISANA. Then, a general description of the route is announced to the user, including intermediate destinations for multi-floor routes, the number of waypoints to the (intermediate) destination and location alert (e.g., "you are in the lobby", or "your destination is on the eighth floor"). ISANA provides verbal guidance for each waypoint and announces the distance to next waypoint in feet or steps. Waypoints are algorithmically computed and adjusted as needed when obstacles are encountered.

6.2 Speech and Audio HMI

ISANA HMI utilizes the Android text-to-audio[2] to convey system feedback such as waypoint guidance, obstacle alerts, and location awareness information. To decrease the cognitive load for the user, an event triggering mechanism is designed to dispatch messages according to the system state machine. Meanwhile, each message is configured with a priority, so that ISANA allows higher priority messages to be delivered on time to supersede the current announcing message.

We implemented a speech-to-text voice recognition module [33] for user input by fine-tuning the CMU PocketSphinx[3] engine. We enhanced the recognition accuracy by creating a limited vocabulary and specified grammar dictionary.

6.3 SmartCane HMI

We designed a SmartCane with tactile input (keypad) and haptic feedback (vibration motors) to provide a robust HMI in noisy environments.

The SmartCane unit, as shown in Fig. 10, is mounted on a standard white cane. The mechatronics functionalities of SmartCane include:

1) A SmartCane handle with a keypad and two buttons is mounted on the standard white cane to select destination candidates and $confirm$, and $reset$ functionalities.
2) A 9-axis IMU is used to track the relative orientation between white cane and the user for accurate heading direction guidance.
3) The two vibration motors on the SmartCane guide the user with correct heading direction.
4) BLE is used for data transmission between ISANA and SmartCane.

The state machine design of the SmartCane is shown in Fig. 11. After the SmartCane starts, it connects with ISANA
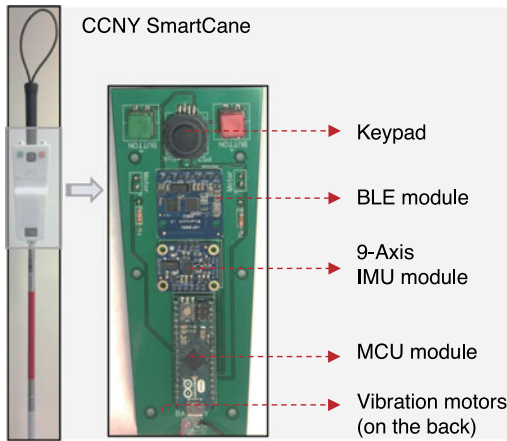
2. http://tinyurl.com/Android-TTS
3. http://cmusphinx.sourceforge.net

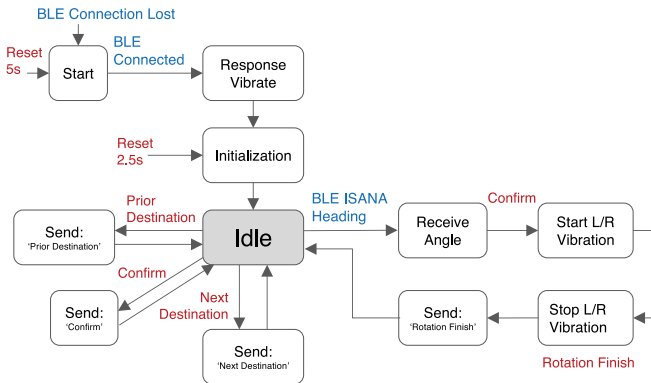Fig. 10. CCNY SmartCane installed on a standard white cane.

Fig. 11. State machine of the SmartCane HMI. The state transition is triggered by two types of events: the blue is from the system and the red is from user tactile input.

via Bluetooth Low Energy (BLE) and the vibration motors are triggered to indicate a successful connection. Then, the state machine falls into the *Idle* state and waits for transition events. When the user presses the keypad or any button, SmartCane delivers these inputs to ISANA.

When ISANA dispatches a heading guidance message to the SmartCane, the user can *Confirm rotation* to track the relative orientation between white cane and the user. The SmartCane conveys accurate direction guidance to the user via haptic feedback. The two vibration motors indicate the directions of turning left or right, its vibration intensity decreases as the user steers to the targeted direction. Finally, vibration stops when the correct heading is reached.

7   EXPERIMENTAL RESULTS

We tested the ISANA and SmartCane system with both blindfolded and blind subjects for its quantitative and qualitative effectiveness in guiding users to their destinations. Also, the semantic map for localization and obstacle detection modules are evaluated in details in this section.

7.1   Map Alignment for Semantic Localization

To verify semantic localization accuracy through the alignment, the trajectories of ISANA in Steinman Hall 6th floor (size around $35m \times 32m$) at CCNY were recorded to evaluate the closed-loop error. The closed-loop trajectory generated using pure visual odometry is drawn in red in Fig. 12, and

Fig. 12. Loop trajectories for ISANA semantic localization versus pure visual odometry.
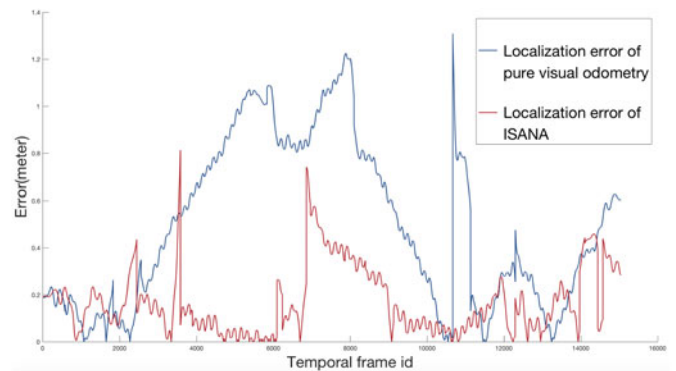

Fig. 13. ISANA semantic localization accuracy versus pure visual odometry accuracy.

the ISANA semantic localization trajectory based on VPS is shown in green. The ground truth is the path at the midpoint of the hallways.

The closed-loop error of both methods are shown in Fig. 13. As one can see, the pure visual odometry accumulates drift with time and leads to larger errors, whereas ISANA semantic localization performs with smaller errors and without drift.

7.2   Obstacle Detection and Motion Estimation

Fig. 14 shows a visualization screenshot of detected obstacles in a hallway on the ISANA App, Different objects are shown as different bounding boxes in front of the user.

The evaluation of the obstacle detection was conducted in a hallway. Fig. 15 shows the obstacles detected from the point cloud. The top two panels indicate the horizontal and vertical projections respectively. The bottom two panels show the VFH weighted histogram of both projections for obstacle-free path directions.

After obstacles are detected, a nearest-neighbor approach [41] was applied to track the objects in subsequent frames.
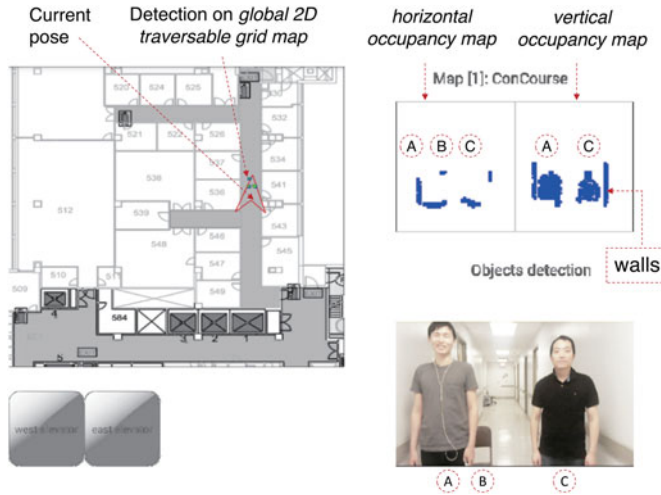
Fig. 14. Obstacle detection results from depth perception projection in ISANA App GUI on a mobile device. On the right side, three objects (A-person, B-chair, and C-person) are projected both horizontally and vertically from the 3D point cloud. On the left side, the objects shown in green with blue outline are the detected object results.
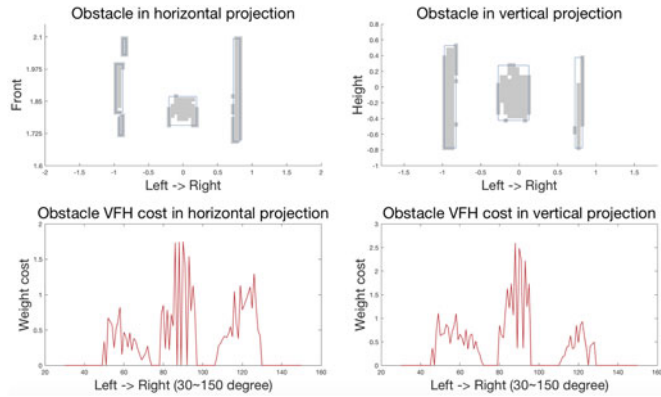

Fig. 15. Left-top: Obstacle detection horizontal projection. The horizontal axis represents the left to right direction in degree, and the vertical axis represents the forward direction in the meter. Left-bottom: obstacle histogram VFH. The horizontal axis is the angular direction in the degrees, and the vertical axis represents the weighted cost of obstacle points about their distance to the user on the horizontal plane. Right side shows the detection in the vertical projection and its VFH.

The tracking metric is defined over the euclidean distance between the centers of gravity of grid ensembles (shown as gray in Fig. 16) representing distinct objects.

Fig. 16 shows the result of continuous frames detection and motion estimation using TSM-KF based on field collected data. $^eP_{i-2}$ is the fused position of the object in time $t = i - 2$ which is marked in yellow. $^eP_{i-1}$ is the fused position of the object in time $t = i - 1$ shown in dark blue. ^pP_i shows the motion prediction position of P_i shown in red. ^mP_i is the measurement of the P_i based on the noise model.

Finally, the ^eP_i is the fused position by updating from ^mP_i based on the prediction of ^pP_i. The circle around each position shows its covariance. The TSM-KF provides a smooth and more accurate motion estimation for obstacle avoidance.

7.3 Navigation with Obstacle Avoidance

If the detected obstacles or the predicted obstacle positions are superimposed on path to the next waypoint, ISANA
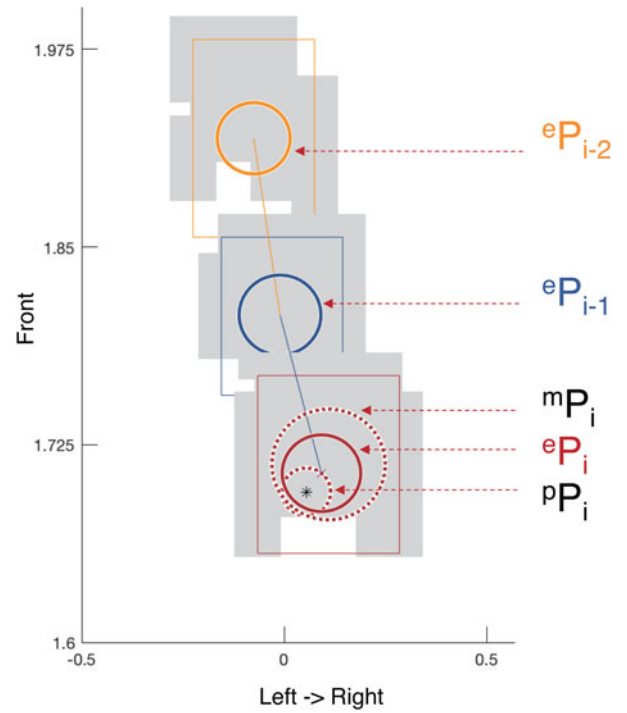

Fig. 16. Obstacle motion prediction and fusion using TSM-KF. ^eP_i is the estimated positions (with covariance ellipsoids) of obstacle in discrete continuous frames (frame t_{i-2} as shown in yellow color, t_{i-1} as dark blue, t_i as red). ^pP_i shows the predicted position with covariance ellipsoid for frame i, ^mP_i shows the measured position and ^eP_i is the updated estimation using KF.

(a) The calculated route using A* and path pruning when there is no detected obstacle.

(b) When ISANA detects any obstacles in front of the user, and it superimposes with the current route, ISANA generates a new route by updating the detection into the global 2D traversable grip map.

(c) When the obstacle moves, ISANA will update the route accordingly for dynamic path planning to avoid obstacle.
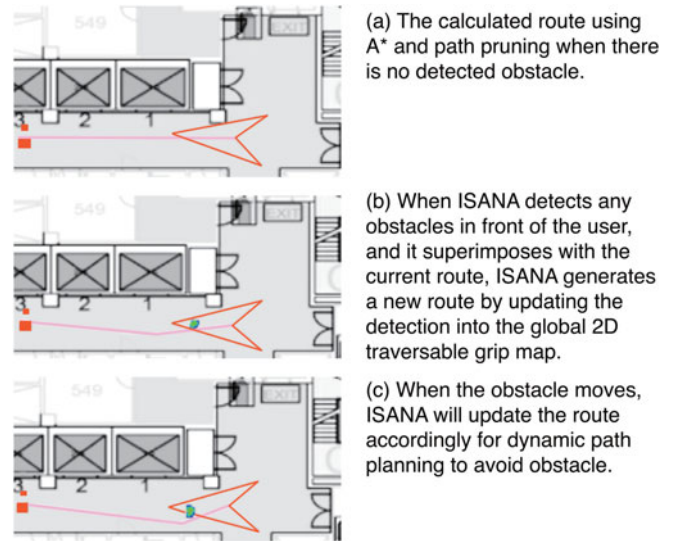
Fig. 17. Real-time obstacle avoidance during navigation.

generates a new path to avoid the obstacles using the path planner [36] based on A^* algorithm. Fig. 17a shows the path when there is no obstacle. When ISANA detects obstacles in front, a new route is generated as shown in Fig. 17b. As the obstacle moves, route is updated to avoid the detected obstacle, as shown in Fig. 17c.

The obstacle avoidance is running along with the assistive navigation, as shown in this demo video.[4]

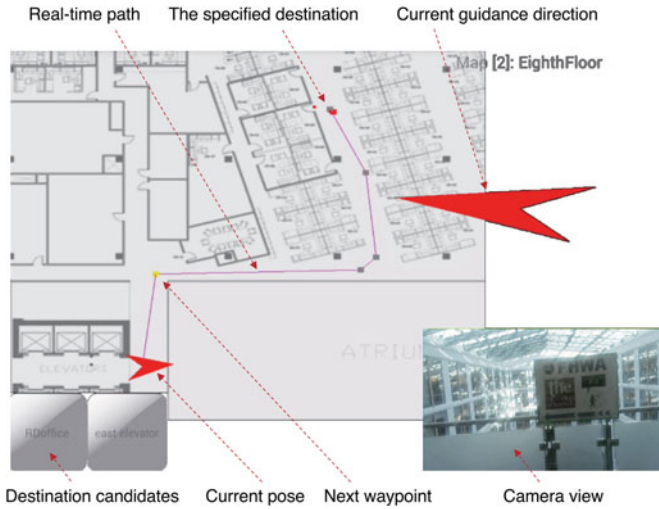4. https://tinyurl.com/ccnyisanaobstacle

Fig. 18. ISANA App GUI, screenshot from field demo at the U.S. Department of Transportation (DOT) headquarter buildings in Washington, D.C.

7.4 System Evaluation

7.4.1 Qualitative Experiments

We initially conducted the ISANA prototyping evaluation in the Steinman Hall at CCNY with blind and blindfolded subjects.

A field demo of ISANA was further performed in U.S. Department of Transportation (DOT) headquarter buildings in Washington, D.C. in an indoor multi-floor environment. A screenshot of the test scene is shown in Fig. 18. The system successfully guided the blind subject to a specified destination with obstacle detection. The user used voice meta keyword *ISANA* to trigger the voice recognition and consequently specified a destination. ISANA computed the path based on the global 2D traversable grid map and guided the user through audio feedback. The field test is shown in this demo video.[5]

7.4.2 Quantitative Experiments

After the DOT test, we added the SmartCane as part of ISANA for accurate heading guidance and haptic feedback. Series of field tests were conducted with blindfolded subjects in Steinman Hall at CCNY to evaluate the effectiveness of ISANA and SmartCane. The journey route from an office room to a stair (around 32 meters) takes 58 seconds for a sighted person who is familiar with the environment under a regular speed. Four blindfolded college students were selected as subjects ($S_{1,2,3,4}$) for both ISANA and ISANA with SmartCane evaluation. These subjects were first trained to get familiar with the system by navigating through a different route. A tested assistive navigation journey using ISANA and SmartCane is shown in this demo video.[6]

The experimental results were evaluated by counting walking errors (which are defined as traveling off course for more than 3 seconds) and traveling time as shown in Table 1. As one can see that the average (Avg.) navigation guidance error (unit: times) was reduced greatly by utilizing SmartCane for accurate heading measurement. Therefore, the traveling

TABLE 1
ISANA Only versus ISANA with SmartCane Evaluation

Criterion	System	S_1	S_2	S_3	S_4	Avg.
Error(times)	ISANA only	3	1	2	2	2.0
Error(times)	with SmartCane	1	0	0	1	0.5
Time(seconds)	ISANA only	203	133	181	186	175.8
Time(seconds)	with SmartCane	176	116	144	159	148.3

time (unit: seconds) was also clearly decreased for the same travel journey.

ISANA runs in real-time on the Google Tango mobile platforms (tested in both Tango Yellowstone and Phab 2 Pro mobile devices). Pose updating is around 100 HZ through visual-inertial odometry. The obstacle detection runs efficiently under 5 HZ during assistive navigation. The period of obstacle avoidance for path updating is adjustable to accommodate user experience, and it is set as $3 \sim 5$ seconds in our experiments. Although the whole system consumes substantial power, it lasts around one and half hours while ISANA is running at full load.

8 CONCLUSIONS AND FUTURE WORK

This paper presents a mobile computing ISANA with SmartCane prototype to assist blind individuals with independent indoor travel. ISANA functionalities include indoor semantic map construction, navigation and wayfinding, obstacle avoidance, and a multi-modal (speech, audio and haptic) user interface. With vision perception situation awareness for the user's surrounding environment and navigation aid, our experimental tests with blindfolded and blind subjects demonstrate the effectiveness of our technology as a useful tool to help blind users with indoor travel.

We conducted comprehensive experimental evaluations on blindfolded and blind subjects in various indoor environments, including both single floor and multi-floor scenarios. Our subjects learned to use ISANA fairly easily. The feedback from subjects indicates that there is still room to improve for better user interface (UI), such as: (1) the speech recognition should be improved for robustness in noisy environments; (2) the audio feedback frequency should be adjustable and customized for different users; (3) the annotation functionality of adding POI landmarks into the semantic map should be easily accessible for blind users.

Future research directions will focus on cognitive understanding and navigation in more complex and cluttered environments, such as transportation terminals.

5. https://tinyurl.com/isanadot
6. https://tinyurl.com/ccnyisanacane

REFERENCES

[1] "Vision impairment and blindness: Fact sheet," *World Health Org.*, 2017. [Online]. Available: http://www.who.int/mediacentre/factsheets/fs282/

[2] A. W. S. Au, C. Feng, S. Valaee, S. Reyes, S. Sorour, S. N. Markowitz, D. Gold, K. Gordon, and M. Eizenman, "Indoor tracking and navigation using received signal strength and compressive sensing on a mobile device," *IEEE Trans. Mobile Comput.*, vol. 12, no. 10, pp. 2050–2062, Oct. 2013.

[3] E. Xu, Z. Ding, and S. Dasgupta, "Target tracking and mobile sensor navigation in wireless sensor networks," *IEEE Trans. Mobile Comput.*, vol. 12, no. 1, pp. 177–186, Jan. 2013.

[4] P.-H. Tseng, Z. Ding, and K.-T. Feng, "Cooperative self-navigation in a mixed LOS and NLOS environment," *IEEE Trans. Mobile Comput.*, vol. 13, no. 2, pp. 350–363, Feb. 2014.

[5] L. Wang, Y. He, W. Liu, N. Jing, J. Wang, and Y. Liu, "On oscillation-free emergency navigation via wireless sensor networks," *IEEE Trans. Mobile Comput.*, vol. 14, no. 10, pp. 2086–2100, Oct. 2015.

[6] C. Wang, H. Lin, and H. Jiang, "CANS: Towards congestion-adaptive and small stretch emergency navigation with wireless sensor networks," *IEEE Trans. Mobile Comput.*, vol. 15, no. 5, pp. 1077–1089, May 2016.

[7] Y. Zhuang, Z. Syed, Y. Li, and N. El-Sheimy, "Evaluation of two WiFi positioning systems based on autonomous crowdsourcing of handheld devices for indoor navigation," *IEEE Trans. Mobile Comput.*, vol. 15, no. 8, pp. 1982–1995, Aug. 2016.

[8] C. Wang, H. Lin, R. Zhang, and H. Jiang, "SEND: A situation-aware emergency navigation algorithm with sensor networks," *IEEE Trans. Mobile Comput.*, vol. 16, no. 4, pp. 1149–1162, Apr. 2017.

[9] C. Zhang, K. P. Subbu, J. Luo, and J. Wu, "GROPING: Geomagnetism and crowdsensing powered indoor navigation," *IEEE Trans. Mobile Comput.*, vol. 14, no. 2, pp. 387–400, Feb. 2015.

[10] Z. Liu, W. Dai, and M. Z. Win, "Mercury: An infrastructure-free system for network localization and navigation," *IEEE Trans. Mobile Comput.*, vol. 17, no. 5, pp. 1119–1133, May 2018.

[11] I. Apostolopoulos, N. Fallah, E. Folmer, and K. E. Bekris, "Integrated online localization and navigation for people with visual impairments using smart phones," *ACM Trans. Interactive Intell. Syst.*, vol. 3, no. 4, 2014, Art. no. 21.

[12] H. He, Y. Li, Y. Guan, and J. Tan, "Wearable ego-motion tracking for blind navigation in indoor environments," *IEEE Trans. Autom. Sci. Eng.*, vol. 12, no. 4, pp. 1181–1190, Oct. 2015.

[13] V. Pradeep, G. Medioni, and J. Weiland, "Robot vision for the visually impaired," in *Proc. IEEE Comput. Soc. Conf. Comput. Vis. Pattern Recognit. Workshops*, 2010, pp. 15–22.

[14] J. Courbon, Y. Mezouar, L. Eck, and P. Martinet, "A generic fisheye camera model for robotic applications," in *Proc. IEEE/RSJ Int. Conf. Intell. Robots Syst.*, 2007, pp. 1683–1688.

[15] K. Terashima, K. Watanabe, Y. Ueno, and Y. Masui, "Auto-tuning control of power assist system based on the estimation of operator's skill level for forward and backward driving of omni-directional wheelchair," in *Proc. IEEE/RSJ Int. Conf. Intell. Robots Syst.*, 2010, pp. 6046–6051.

[16] Y. H. Lee and G. Medioni, "RGB-D camera based wearable navigation system for the visually impaired," *Comput. Vis. Image Understanding*, vol. 149, pp. 3–20, 2016.

[17] "Cydalion: Assistive navigation app for people with visual impairments," Illinois State Univ., 2016. [Online]. Available: http://cydalion.com/

[18] "Augmented reality indoor navigation," *Cologne Intell.*, 2017. [Online]. Available: https://www.cologne-intelligence.de/english/augmented-reality-indoor-navigation/

[19] B. Schilit, N. Adams, and R. Want, "Context-aware computing applications," in *Proc. 1st Workshop Mobile Comput. Syst. Appl.*, 1994, pp. 85–90.

[20] W. S. Gribble, R. L. Browning, M. Hewett, E. Remolina, and B. J. Kuipers, "Integrating vision and spatial reasoning for assistive navigation," in *Assistive Technology and Artificial Intelligence*. Berlin, Germany: Springer, 1998, pp. 179–193.

[21] F. Lyardet, J. Grimmer, and M. Muhlhauser, "CoINS: Context sensitive indoor navigation system," in *Proc. 8th IEEE Int. Symp. Multimedia*, 2006, pp. 209–218.

[22] F. Lyardet, D. W. Szeto, and E. Aitenbichler, "Context-aware indoor navigation," in *Ambient Intelligence*. Berlin, Germany: Springer, 2008, pp. 290–307.

[23] I. Afyouni, R. Cyril, and C. Christophe, "Spatial models for context-aware indoor navigation systems: A survey," *J. Spatial Inf. Sci.*, vol. 1, no. 4, pp. 85–123, 2012.

[24] I. Afyouni, "Knowledge representation and management in indoor mobile environments," Ph.D. dissertation, Dept. Computer Science, The Naval Academy Research Institute, Université de Bretagne occidentale-Brest, Brest, France, 2013.

[25] D. A. Bell, S. P. Levine, Y. Koren, L. A. Jaros, and J. Borenstein, "Shared control of the NavChair obstacle avoiding wheelchair," in *Proc. TITLE Eng. ADA Vis. Reality Tech. Conf.*, vol. 13, p. 384, 1993.

[26] D. Bell, J. Borenstein, S. P. Levine, Y. Koren, L. Jaros et al., "An assistive navigation system for wheelchairs based upon mobile robot obstacle avoidance," in *Proc. IEEE Int. Conf. Robot. Autom.*, 1994, pp. 2018–2022.

[27] N. Ortigosa, S. Morillas, and G. Peris-Fajarn és, "Obstacle-free pathway detection by means of depth maps," *J. Intell. Robot. Syst.*, vol. 63, no. 1, pp. 115–129, 2011.

[28] Y. Lee and G. Medioni, "Wearable RGBD indoor navigation system for the blind," in *Proc. Eur. Conf. Comput. Vis.*, 2014, pp. 493–508.

[29] R. Jafri and M. M. Khan, "Obstacle detection and avoidance for the visually impaired in indoors environments using Googles project Tango device," in *Proc. Int. Conf. Comput. Helping People Special Needs*, 2016, pp. 179–185.

[30] R. Jafri, R. L. Campos, S. A. Ali, and H. R. Arabnia, "Utilizing the Google project Tango tablet development kit and the unity engine for image and infrared data-based obstacle detection for the visually impaired," in *Proc. Int. Conf. Health Inform. Med. Syst.*, 2016, pp. 163–164.

[31] A. Alahi, R. Ortiz, and P. Vandergheynst, "FREAK: Fast retina keypoint," in *Proc. IEEE Conf. Comput. Vis. Pattern Recognit.*, 2012, pp. 510–517.

[32] J. P. Muñoz, B. Li, X. Rong, J. Xiao, Y. Tian, A. Arditi, and N. Chappaqua, "Demo: Assisting visually impaired people navigate indoors," in *Proc. Int. Joint Conf. Artif. Intell.*, 2016, pp. 4260–4261.

[33] X. Rong, B. Li, J. P. Muñoz, J. Xiao, A. Arditi, and Y. Tian, "Guided text spotting for assistive blind navigation in unfamiliar indoor environments," in *Proc. Int. Symp. Visual Comput.*, 2016, pp. 11–22.

[34] Q. Chen, M. Khan, C. Tsangouri, C. Yang, B. Li, J. Xiao, and Z. Zhu, "CCNY smart cane," in *Proc. IEEE Int. Conf. CYBER Technol. Autom. Control Intell. Syst.*, 2017.

[35] B. Li, J. P. Muñoz, X. Rong, J. Xiao, Y. Tian, and A. Arditi, "ISANA: Wearable context-aware indoor assistive navigation with obstacle avoidance for the blind," in *Proc. Eur. Conf. Comput. Vis.*, 2016, pp. 448–462.

[36] J. P. Muñoz, B. Li, X. Rong, J. Xiao, Y. Tian, and A. Arditi, "An assistive indoor navigation system for the visually impaired in multi-floor environments," in *Proc. IEEE Int. Conf. CYBER Technol. Autom. Control Intell. Syst.*, 2017.

[37] B. Li, X. Zhang, J. P. Muñoz, J. Xiao, X. Rong, and Y. Tian, "Assisting blind people to avoid obstacles: A wearable obstacle stereo feedback system based on 3D detection," in *Proc. IEEE Int. Conf. Robot. Biomimetics*, 2015, pp. 2307–2311.

[38] L. Cabaret and L. Lacassagne, "What is the world's fastest connected component labeling algorithm?" in *Proc. IEEE Int. Workshop Signal Process. Syst.*, 2014, Art. no. 6.

[39] A. Arditi and Y. Tian, "User interface preferences in the design of a camera-based navigation and wayfinding aid," *J. Visual Impairment Blindness (Online)*, vol. 107, no. 2, 2013, Art. no. 118.

[40] R. Golledge, R. Klatzky, J. Loomis, and J. Marston, "Stated preferences for components of a personal guidance system for nonvisual navigation," *J. Visual Impairment Blindness*, vol. 98, no. 03, pp. 135–147, 2004.

[41] E. Prassler, J. Scholz, and P. Fiorini, "A robotics wheelchair for crowded public environment," *IEEE Robot. Autom. Mag.*, vol. 8, no. 1, pp. 38–45, Mar. 2001.
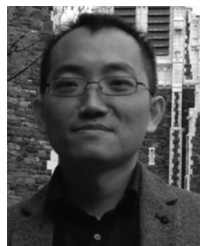
Bing Li received the BE degree from Beijing Forestry University, in 2006, the ME degree from Beihang University, Beijing, China, in 2009, and the PhD degree from City College (CCNY), City University of New York (CUNY), in 2018. Previously, he worked for the China Academy of Telecommunication Technology (Datang Telecomm), HERE North America LLC, and IBM. His PhD research focused on vision-based intelligent situation awareness and navigation aid (ISANA) for the visually impaired. His current research interests include robotics, computer vision, machine learning, 3D semantic SLAM, assistive navigation, and robot inspection. He is a member of the IEEE.

Juan Pablo Muñoz received the graduate magna cum laude degree from Brooklyn College with the BA degree in philosophy, and membership in Phi Beta Kappa. He received the MS degree in computer science from the Grove School of Engineering, City College of New York, and the PhD degree in computer science from the City University of New York. He is currently a research scientist with the Intel Corporation. His research includes the development of frameworks for video analytics that can be deployed at large scale. Previously, he successfully led the development of localization systems for assisting visually impaired people to navigate indoors, and designed and implemented an award winning prototype to combat the spread of Zika virus using state-of-the-art computer vision techniques and citizen science. He is a member of the IEEE.

Xuejian Rong received the BE degree from the Nanjing University of Aeronautics and Astronautics with honors thesis, in 2013. He is working toward the PhD degree at the City University of New York advised by Yingli Tian. His research interests include visual recognition and machine learning with a focus on deep learning based scene text extraction and understanding. He also worked in the areas of image degradation removal such as image deblurring and denoising.
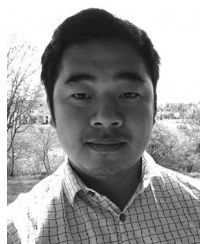
Qingtian Chen received the BE degree in electrical engineering from CCNY, in 2017. He founded the FIRST Robotics Club at CCNY to inspire others to explore the field of robotics. During his BE study, he conducted robotics and robot operating system (ROS) research in Aachen, Germany and the CCNY Robotics Lab. Currently, he is working for the Naval Nuclear Laboratory as an electrical engineer.

Jizhong Xiao received the BS and MS degrees from the East China Institute of Technology, Nanjing, China, in 1990 and 1993, respectively, the ME degree from Nanyang Technological University, Singapore, in 1999, and the PhD degree from Michigan State University, in 2002. He is a professor and PhD program advisor with the Department of Electrical Engineering of CCNY. He started the Robotics Research Program with CCNY, in 2002 and is the founding director of the CCNY Robotics Lab. His current research interests include robotics and control, cyber-physical systems, autonomous navigation and 3D simultaneous localization and mapping (SLAM), realtime and embedded computing, assistive technology, multi-agent systems, and swarm robotics. He has published more than 160 research articles in peer reviewed journal and conferences. He is a senior member of the IEEE.

Yingli Tian (M'99-SM'01-F'18) received the BS and MS degrees from Tianjin University, China, in 1987 and 1990, respectively, and the PhD degree from the Chinese University of Hong Kong, Hong Kong, in 1996. After holding a faculty position with the National Laboratory of Pattern Recognition, Chinese Academy of Sciences, Beijing, she joined Carnegie Mellon University, in 1998, where she was a postdoctoral fellow with the Robotics Institute. She then worked as a research staff member in the IBM T. J. Watson Research Center from 2001 to 2008. She is one of the inventors of the IBM Smart Surveillance Solutions. She has been a professor with the Department of Electrical Engineering, City College, and the Department of Computer Science, Graduate Center, City University of New York, since 2008. Her current research focuses on a wide range of computer vision problems from object recognition, scene understanding, to human behavior analysis, facial expression recognition, and assistive technology. She is a fellow of the IEEE.

Aries Arditi received the PhD degree from NYU and postdoctoral training with Northwestern University and NYU, after which he directed and conducted vision science with Lighthouse Guild and the IBM Watson Research Center. He has served as president of the International Society of Low Vision Research and Rehabilitation, as editor-in-chief of the *Journal Visual Impairment Research*, and on numerous U.S. government committees and panels relating to vision science. He is a research diplomate and fellow of the American Academy of Optometry and a fellow of the American Psychological Society. He is author of more than 150 scientific publications. With wide-ranging interests in vision science, accessibility, and vision rehabilitation, he now conducts research with Visibility Metrics LLC, and develops clinical vision tests through the Mars Perceptrix Corporation.

Mohammed Yousuf received the BS degree in electronics and communication engineering, and the MS degree in computer engineering. He is a program manager for the Accessible Transportation Technology Research Initiative (ATTRI). He is involved in research on new technology solutions for wayfinding and navigation guidance for built and pedestrian environments. He is also involved in research related to emerging technologies including wireless communications, mapping, positioning and navigation, robotics, and artificial intelligence for surface transportation. Prior to joining FHWA, he worked with General Motors and Chrysler Group. He served as the expert advisor to the Transportation and Technology Subcommittee, the National Taskforce on Workforce Development for People with Disabilities and is the co-chair of the Technology Subcommittee, Transportation Research Board Committee on Accessible Transportation and Mobility. He is a member of the Technology for Aging Taskforce, Autism Cares Interagency Workgroup, Intelligent Robotics & Autonomous Systems (IRAS) Interagency Workgroup, Interagency Committee of Disability Research (ICDR), and Transportation Research Board Committee on Automated Vehicles and a former member of the FCC Disability Advisory Committee. He has a patent on wireless multiplex systems and methods for controlling devices in vehicle.

▷ **For more information on this or any other computing topic, please visit our Digital Library at** www.computer.org/publications/dlib.